14th Australasian Fluid Mechanics Conference
Adelaide University, Adelaide, Australia
10-14 December 2001

Wind wave evolution in finite depth water

I.R. Young[1] and A.V. Babanin[2]

[1]Faculty of Engineering, Computer & Mathematical Sciences
Adelaide University, Adelaide, South Australia, 5005 AUSTRALIA

[2]Department of Civil & Environmental Engineering
Adelaide University, Adelaide, South Australia, 5005 AUSTRALIA

Abstract

This paper presents recent research aimed at developing a detailed predictive capability for wind generated ocean waves in shallow coastal waters. The detailed evolution of the directional spectrum, and measurements of the source terms responsible for this evolution are presented.

Introduction

Wind generated ocean waves are important for a number of reasons. From an engineering viewpoint, they represent the major loading on coastal and offshore structures. From the environmental context, they have a governing role in the stability of coastlines and the flooding of near-coastal regions during storm condition. Wind generated waves also largely govern the aerodynamic roughness of the ocean surface and hence play a major role in determining the fluxes of heat, energy, momentum and possibly carbon dioxide across the ocean surface. Thus accurate prediction of ocean wave conditions may also be a key variable in predicting long-term climate.

The study of gravity waves has been a fertile area of fluid mechanics for many centuries. Our abilities to predict the generation and evolution of ocean waves on a global or regional scale only started to develop in the 1950s (Gelci et al, 1956 [4]). The sophistication of such models has increased as both computing power grew and our understanding of the, often complex, nonlinear processes governing wind-wave evolution increased. This development has culminated in the introduction of 3rd Generation spectral models, capable of predicting wave fields on either a global of regional scale (WAMDI, 1988 [10]).

Despite the significant developments which have occurred in this area, the resulting models have largely been confined to areas of deep water, where the influences of finite depth can be ignored. Although deep-water regions include the vast majority of the world's oceans, it is in the relatively small shallow coastal regions where the bulk of human activity is concentrated. Until recently, both the form of wind generated waves in shallow coastal regions and the mechanisms responsible for their evolution have been poorly understood. This paper describes a number of integrated field research projects aimed at addressing this lack of knowledge.

Governing Equations

For the simplifying case of a constant water depth, the evolution of the directional wave spectrum can be described by the energy balance equation

$$\frac{\partial F}{\partial t} + \mathbf{C_g} \cdot \nabla F = S_{tot} \qquad (1)$$

where F is the directional wave spectrum, t is time, $\mathbf{C_g}$ is the group velocity and S_{tot} is a source term which represents all processes which transfer energy to, from or between components of the wave spectrum F. To first order, S_{tot} can be represented as the sum of a number of separate processes

$$S_{tot} = S_{in} + S_{wc} + S_{bf} + S_{4nl} + S_{3nl} \qquad (2)$$

where each of the terms represents a specific physical process

$S_{in} \equiv$ input from the wind

$S_{wc} \equiv$ dissipation due to white-cap breaking at the surface

$S_{bf} \equiv$ dissipation due to friction with the bottom

$S_{4nl} \equiv$ 4-wave resonant non-linear interactions between components in the spectrum

$S_{3nl} \equiv$ 3-wave or triad interactions between components of the spectrum

Experimental Description

Little detailed knowledge was available on either the form of the wave spectrum, F or of the individual source terms in (2) for finite depth conditions. As a result, a detailed set of field experiments were conducted at Lake George, near Canberra, Australia. Lake George is approximately 20 km in length by 10 km wide. It has a remarkably flat bottom, with a depth that varies seasonally.

Two major sets of experiments were conducted at Lake George. The first of these involved measuring the evolution of the wave spectrum as a function of fetch (distance from shore), under conditions were the wind was constant and blew approximately perpendicular to the shoreline (often termed *Fetch Limited Conditions*). Effectively, such data yields the evolution of the spectrum, as shown on the left side of (1). The second set of experiments involved detailed measurements of the individual source terms in (2), that is, the right side of (1). Analysis of the data should close the balance in (1).

Non-dimensional growth curves

Dimensional analysis indicates that the evolution of the total wave energy and of a representative wave frequency can be expressed in terms of a small number of non-dimensional parameters. Based on the very extensive Lake George data set, Young and Verhagen (1996a) [13] have shown that the non-dimensional energy, ε and non-dimensional peak frequency, ν can be expressed in terms of the non-dimensional fetch, χ and non-dimensional water depth, δ. Examples of these relationships are shown in Figures 1 and 2.

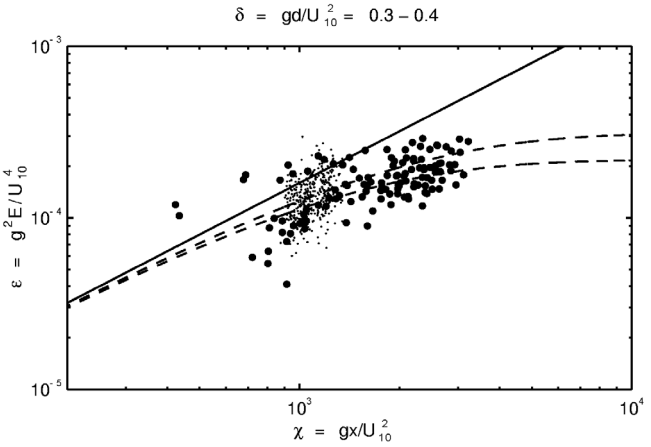

Figure 1. Scatter plot of the non-dimensional energy, ε against non-dimensional fetch, χ. Only data with values of non-dimensional depth, δ between 0.3 and 0.4 are shown. Equation (3) is shown for these two extremes of δ by the dashed lines and the deep-water asymptote by the solid line.

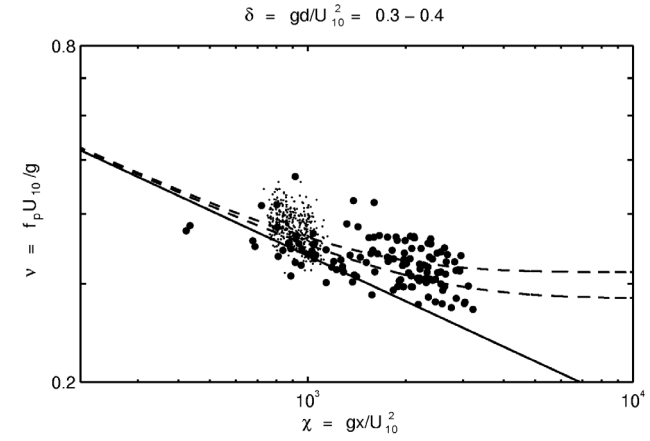

Figure 2. Scatter plot of the non-dimensional frequency, ν against non-dimensional fetch, χ. Only data with values of non-dimensional depth, δ between 0.3 and 0.4 are shown. Equation (6) is shown for these two extremes of δ by the dashed lines and the deep-water asymptote by the solid line.

Young and Verhagen (1996a) [13] represented these data by a relationships of the form

$$\varepsilon = 3.64\times10^{-3}\left\{\tanh A_1 \tanh\left[\frac{B_1}{\tanh A_1}\right]\right\}^{1.74} \quad (3)$$

where

$$A_1 = 0.493\delta^{0.75} \quad (4)$$

$$B_1 = 3.13\times10^{-3}\chi^{0.57} \quad (5)$$

and

$$\nu = 0.133\left\{\tanh A_2 \tanh\left[\frac{B_2}{\tanh A_2}\right]\right\}^{-0.37} \quad (6)$$

$$A_2 = 0.331\delta^{1.01} \quad (7)$$

$$B_2 = 5.215\times10^{-4}\chi^{0.73} \quad (8)$$

In these relationships the non-dimensional variables are defined as $\varepsilon = g^2E/U_{10}^4$, $\nu = f_pU_{10}/g$ and $\delta = gd/U_{10}^2$, where g is gravitational acceleration, E is the variance or total energy of the water surface elevation, U_{10} is the wind speed, f_p is the frequency of the spectral peak and d is the water depth.

Equations (3) describes the evolution of the total energy and spectral peak frequency as a function of fetch, wind speed and water depth, but yield no information about the detailed evolution of the spectrum.

Spectral evolution

Young and Verhagen (1996b) [14] compiled an extensive data set of the evolution of the one-dimensional frequency spectrum $F(f)$, an example of which is shown in Figure 3.

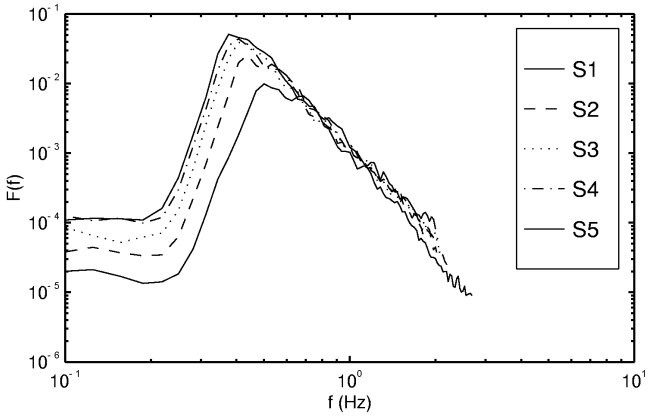

Figure 3. An example of the development of the finite depth wave spectrum with fetch. The stations where the measurements were made are labeled S1 to S5 (increasing fetch from 1.3km to 6.7km). The wind speed was 10.8 m/s.

Young and Verhagen (1996b) [14] parameterized these results in terms of the well-known JONSWAP spectral form (Hasselmann et al, 1973 [5])

$$F(f) = \alpha g^2\left(2\pi\right)^{-4} f^{-5}\exp\left[-\frac{5}{4}\left(\frac{f}{f_p}\right)^{-4}\right] \cdot \gamma^{\exp\left[\frac{-\left(f-f_p\right)^2}{2\sigma^2 f_p^2}\right]} \cdot \Phi \quad (9)$$

where Φ is a Jacobean.

Young and Verhagen (1996b) could find no systematic trends within their data for the values of γ and σ and adopted their mean values $\gamma = 2.70$ and $\sigma = 0.12$. They found that α could be represented in terms of the non-dimensional wave number $\kappa = U_{10}^2k_p/g$, where k_p is the wave number of the spectral peak, as

$$\alpha = 0.0091\kappa^{0.24} \quad (10)$$

Equation (9) appears to indicate a spectrum with a high frequency face proportional to f^{-5}, but inclusion of the Jacobean means that the magnitude of the exponent decreases as the water depth decreases, approaching f^{-3} in very shallow

water. The data of Young and Verhagen (1996b) [14] clearly showed this evolution.

Directional spreading

As part of the Lake George experiments Young et al (1996) [15] deployed a high-resolution directional array, capable of determining the directional properties of the waves. In keeping with previous deep-water representations, Young et al (1996) [15] represented their data in the form

$$F(f,\theta) = A(f)F(f)\cos^{2s}\left(\frac{\theta}{2}\right) \qquad (11)$$

where θ is the direction of wave propagation and the exponent s determines the width of the directional spreading (high vales of s correspond to narrow spreading). $A(f)$ is a normalizing function. Figure 4 shows values of s as a function of the normalized frequency f / f_p and non-dimensional depth parameter $k_p d$.

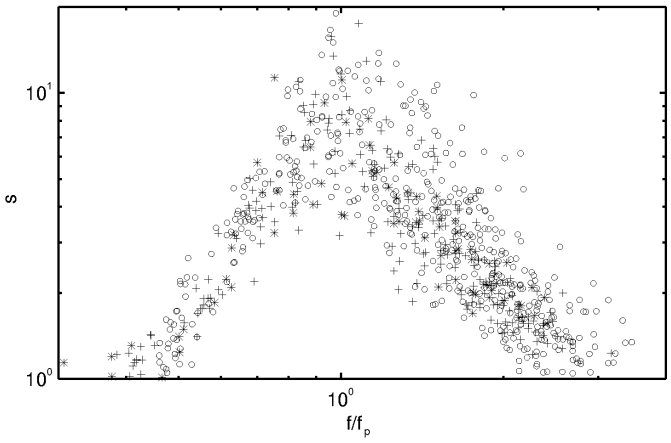

Figure 4. Values of the directional exponent s as a function of the normalized frequency f / f_p . Values have been partitioned based on the relative depth parameter, $k_p d$. $1.0 < k_p d < 1.5 - \text{'}\circ\text{'}, 1.5 < k_p d < 2.0 - \text{'}+\text{'}, k_p d > 2.0 - \text{'}*\text{'}$.

These results have been parameterized as

$$s = \begin{cases} 11\left(\frac{f}{f_p}\right)^{2.7} & for \quad f < f_p \\ 11\left(\frac{f}{f_p}\right)^{-2.4} & for \quad f \geq f_p \end{cases} \qquad (12)$$

Further analysis by Young et al (1995) [12] and more recently by Wang and Hwang (2001) [11] has revealed that the directional spreading may be more complex than indicated by (12). These analyses indicate that the uni-modal for represented by (12) is reasonable to first order, but that the detailed spreading may, in fact, be bi-modal with slightly more energy propagating at angles to the wind, than in the wind direction.

A summary of finite-depth evolution

The data set described above presents a consistent picture of the evolution of the finite depth wave spectrum with fetch. As the fetch increases, the total energy of the spectrum increases and the peak frequency decreases. At long fetch, this evolution ceases as a result of interaction with the bottom. As a result, this asymptotic limit to growth decreases as the water depth decreases. In comparison to deep-water spectra, the one-dimensional spectral form for finite depth waves has a high frequency face which decays more slowly. The directional spreading of finite depth spectra is similar to that of their deep-water counter parts, although the spreading is possibly a little broader. Young et al (1996) [15] speculated that the apparently broader directional spreading in finite depth situations may be due to the behaviour of S_{4nl} in such situations. In finite depth situations S_{4nl} is capable of coupling spectral components more widely separated in frequency and direction space, thus possibly leading to a more isotropic spectral form. The detailed interaction of the various source terms in finite depth situations is, however, still to be fully understood.

The formulations presented above provide a reasonably accurate representation of the evolution of the directional wave spectrum with fetch, that is dF / dt , or the right hand side of (1).

Determination of source terms

Following the experimental campaign aimed at determining the spectral evolution, a separate program was mounted to determine the source terms on the right hand side of (1). An integrated set of measurements in the atmospheric and sub-surface boundary layers as well as on the surface itself were conducted.

The experimental site developed for these experiments included an observational platform, with a shelter to accommodate electronics and equipment as well as researchers during observations. An anemometer mast, housing 3 wind probes at 10 m and 5.65 m elevations over the water surface, was erected 10 m from the platform. Another anemometer mast, housing 5 wind probes at four heights closer to the surface, was set 6 m off the bridge to ensure undisturbed airflow for these lower anemometers. The bridge was used for the majority of the wave measurements. Two shelters constructed onshore provided basic storage and accommodation for researchers during their stay at the site. The location had vehicular access, a simple offshore bathymetry and water of approximately 0.5 m depth within 50 m of the shoreline, ideal for the objectives of the shallow water study. The platform, located approximately 50 m offshore was shore-connected with an elevated walkway and was thus accessible in any weather conditions. Computer facilities allowed for preliminary data analysis to be performed on site, though the main data processing was conducted subsequently. The full experimental facility is shown in Figures 5 and 6.

To measure "white-capping" dissipation, four different but integrated instrument systems were employed. Since individual waves naturally change their heights whilst propagating within irregular wind wave groups, direct in situ estimates of energy lost by breaking were obtained in terms of the integrated group energy, measured with an array of capacitance wave probes. The array also allowed measurement of directional wave spectra.

Figure 5. A view of the observation platform from the shore. The elevated walkway can be seen in the foreground, with the accommodation module visible on the platform.

Figure 6. View of the observation platform taken from an offshore location. The two anemometer masts can be seen to the left. The major measurement bridge, where most of the measurements were conducted joins the platform at the right to the anemometer masts. A wave gauge is seen in the foreground.

Three additional mobile wave probes were positioned to measure spatial decay of breaking wave groups. An observer also marked data records electronically, in response to visual observations of breaking. Facilities for quick in situ calibrations of the wave probes were available. Three Acoustic Doppler Current Meters (ADV) were employed for simultaneous measurement of dissipation rates through the water column in the vicinity of the array. During the experiment (termed AUSWEX), these measurements of the turbulence were supplemented by "Dopbeam" measurements of wave-number velocity spectra. The Dopbeam was provided by Kendall Melville of the Scripps Institution of Oceanography, USA for the period of the experiment. An underwater hydrophone, the output of which is related to both the strength and dimension of breakers, was located on the bottom beneath the array. Video recording of the surface spot around the array was used to identify breaking events and to supply information on the spatial dimensions of white-capping. The logging of all systems, including the video, was synchronized.

Simultaneously, measurements in the atmospheric boundary layer were also conducted. The anemometer masts had six cup anemometers logarithmically spaced from 0.5 m to 10 m and two wind direction vanes. The data logging was synchronized with the wave and breaking recordings. In addition to the wind profile measurements, a sonic anemometer was also deployed on one mast to provide direct estimates of the momentum fluxes. A wave following pressure system, developed and operated by Mark Donelan from the University of Miami, USA, was deployed during AUSWEX to explore wave-induced stresses and pressure fluctuations in the atmosphere.

It was initially proposed to measure the bottom shear stress with a bottom mounted shear plate. Preliminary tests, however, indicated that the mud bottom of the lake was not suitable for this instrument. Hence, a high precision traversing system was used to measure vertical velocity profiles in the bottom boundary layer with one of the ADVs, the measurement volume of which was reduced to 1 mm for this purpose. To determine bottom friction estimates, precise laboratory experiments were conducted. These measurements were designed to determine accurate values of the bottom roughness and friction parameters for the cohesive Lake George mud to be used in further estimates of the bottom dissipation.

Full analysis of the data will include a modelling phase, in which the EXACT-NL model of Hasselmann will be used. The model will be forced with the source terms measured at the experimental site and spectral evolution compared with the comprehensive data previously obtained at the Lake George site (Young et al., 1996).

Data from the Lake George site were obtained for three years, including the intensive AUSWEX period. A database, containing hundreds of hours of wave, wind, air turbulence, sub-surface currents and turbulence, under-water sound, humidity, air and water temperatures and other records, as well as photographic images of the surface, was prepared, documented and archived on seven CDs. About 90 hours of relevant video and hydrophone sound records, with synchronizing time code, were stored on two sets of 40 Super-VHS video tapes.

The joint AUSWEX experiment was carried out from 14 August to 18 September, 1999. The data acquired comprise numerous synchronized records by the wave array, anemometer masts, sonic anemometer, three acoustic doppler velocimeters (ADV) located at different levels in the water column, video camera, hydrophone, humidity and temperature probes, as well as by the Dopbeam, which was traversed to different depths, and by the wave follower. These data comprise four CDs and about 45 hours of video and hydrophone sound records.

A number of laboratory tests were conducted to clarify fine details of the physical processes and the complex behaviour of measurement devices.

Atmospheric Input

The atmospheric input to the wave field can be measured directly from the atmospheric pressure - water surface slope correlation, measured at the water surface. Hence, measurements need to be made of the extremely small wave induced air flow pressure fluctuations, very close to the moving water surface. In the present experiments, this was achieved using an electrically driven servo-feedback wave follower. This system held a disc shaped pressure probe (calibrated to measure static pressure), a fixed distance above the water surface. The system was extensively tested and was found to have a "flat" transfer function for frequencies lower than 5 Hz.

Despite the excellent frequency response of the wave follower, the pressure signal needs to be carefully corrected for spurious fluctuations introduced by the motion of the pressure probe and associated tubing and for the frequency response of the tubing (amplitude and phase).

Based on these data, the atmospheric input source term was represented in a parametric form as:

$$S_{in}(f) = \frac{\rho_a}{\rho_w} g\gamma(f) fF(f) \qquad (13)$$

where, $\gamma(f)$ is a spectral growth increment function

$$\gamma(f) = a\left(\frac{U_{\lambda(f)/2}}{c} - 1\right)^2 \qquad (14)$$

ρ_a and ρ_w are the densities of air and water respectively, c is the wave phase speed and $U_{\lambda/2}$ is the wind velocity, measured at a height equal to one-half wavelength above the mean water surface. Equations (13) and (14) can be used to directly calculate the wind input based on the wave spectrum and the local mean wind information.

The coefficient *a,* was calculated from the Lake George data as 0.14. Donelan (1999) [3], however, based on laboratory data, obtained a value 0.28, twice as large as the present data set. Hence, it appears that this coefficient is not a universal constant, but a function of other parameters.

Further investigation indicated that a is a function of the wave breaking activity. Figure 7 shows an example of a typical wave record, and the associated atmospheric input. The sharp-crested waves in the 2nd, 7th and 12th seconds in the top plot were identified as downwind propagating breakers by means of the synchronized video records. These breakers are also detected by the bottom pressure sensor (bottom plot), which was subsequently used to identify breaking events. The middle subplot shows local running average values of the momentum flux from the wind to the waves. There is clear enhancement of the input, associated with the breakers.

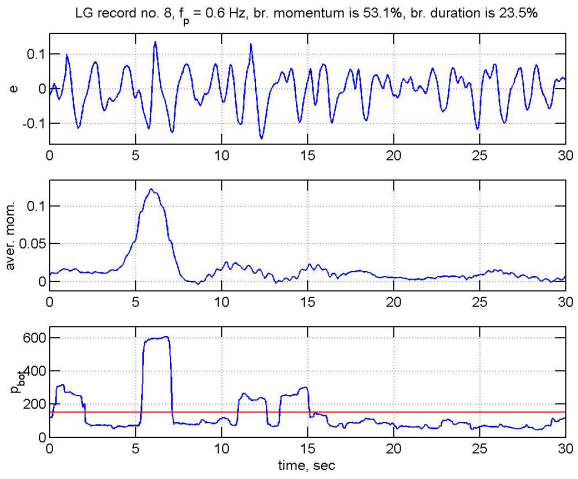

Figure 7. A typical water surface elevation record (top). Breaking waves occur at the 2nd, 7th and 12th seconds. The middle panel shows the atmospheric input to the waves, with clear enhancement associated with the breaking waves. The bottom panel shows a running average of the bottom pressure.

The enhancement associated with the breaking events in Figure 7 appears to be associated with atmospheric flow separation which occurs above breaking waves. The separation "bubble" significantly changes the phase difference between the pressure and the water surface elevation, thus enhancing input. A full understanding of the detailed dependence of a on the breaking activity is presently being investigated.

White-cap dissipation

Of all the source functions responsible for wave evolution, the "white-capping" dissipation term is the most poorly understood. Hence, initial analysis of the extensive Lake George data set focused on the study of the properties of wave breaking. The major goals were:

1. to find reliable techniques for the detection of breakers in the records by instrumental means and without the use of subjective criteria and
2. to study breaking statistics as a function of spectral properties

The concentration on spectral measures of breaking statistics was aimed at implementation in spectral wave prediction models.

The acoustic signature of the breakers, as recorded by the hydrophone has been used as an objective measure of breaking. Spectrograms below (Figure 8) clearly show breaking events as local maxima which span a frequency bandwidth in excess of 4 *KHz*. The breaking events shown in the spectrograms have been

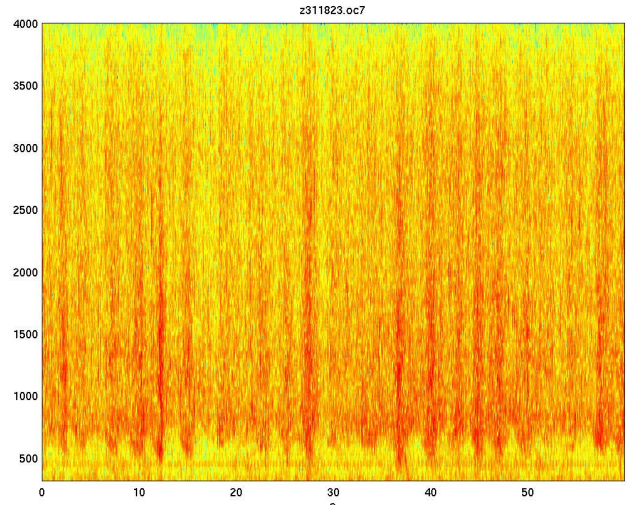

Figure 8. One minute spectrogram of the wave acoustic data. The signatures of breaking waves can clearly be seen as the local maxima (dark regions). An episode of 14 breaking waves which occurred under U_{10}=19.8 m/s wind at f_p = 0.37 Hz peak frequency and H_s = 0.46 m significant wave height.

Banner et al. (2000) [1] have investigated breaking in deep water and found the probability of breaking is closely associated with the hydrodynamic deformation of wave groups. Using the Lake George data set, Babanin et al. (2001) [2] have extended this concept to finite depth conditions.

They have represented the probability of breaking, b_T as:

$$b_T = 6.16\left[\left(\xi - 0.55\right)\left(1 + \frac{H_s}{d}\right)\left(1+\Delta\right)\left(1+\nu\right)\right]^{1.91} \qquad (15)$$

where ξ is the significant steepness of the spectral peak

$$\xi = \frac{H_p k_p}{2} \tag{16}$$

and $H_p = 4\left[\int_{0.7f_p}^{1.3f_p} F(f)df\right]^{1/2}$. $\Delta = u_s / u_0$ is the ratio of the wind induced shear current to the maximum orbital velocity, which has been approximated by $\Delta = 0.01U_{10}/(\varepsilon C_p)$. The Lake George data, as presented by Babanin et al. (2001) [2] is remarkably well represented by (15), as shown in Figure 9.

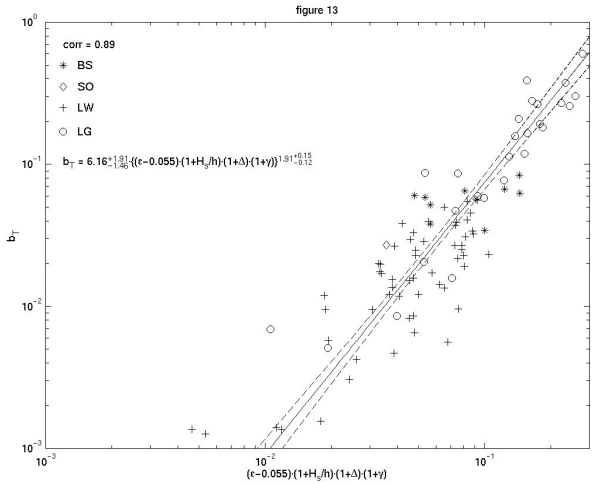

Figure 9. The probability of breaking as a function of the parameters represented in (15). Data are presented from both deep water and finite depth situations. (after Babanin et al., 2001 [2])

An understanding of the breaking probability and its dependence on other physical parameters is important, and provides an essential first step in determining the dissipation source term. It does not, however, provide a direct measure of energy loss during breaking events. Such estimates can be made from measurements of the total energy dissipation in the water column.

At Lake George, two different devices, the standard SonTek ADV and the Dopbeam (Veron and Melville, 1999 [9]), were used to obtain local dissipation rates by measuring Kolmogorov turbulence spectra. The ADV works only in the frequency domain, whereas the Dopbeam provides both frequency and wavenumber spectra of the velocity fluctuations. Once the local dissipation rates are obtained at a number of water depths, they need to be integrated over the whole water depth to provide an estimate of the total dissipation per unit of wavy surface. Therefore, knowledge of the depth profile of the dissipation is required, which is impossible to measure precisely using devices such as the ADV or Dopbeam, particularly very close to the surface. The study by Terray et al. (1996) [8] provided a parameterization of the dissipation profile as a z^{-2} function of the water depth z. The z^{-2} dependence was confirmed at Lake George, however, the parameterization was revised in terms of the dissipation behaviour near the surface and the wind influence on the transition from the linear wall layer to the quadratic function. Clearly, this form of dependence cannot be extended to $z = 0$. The following, piecewise relationship was found suitable for the Lake George data set to model the dissipation profile:

$$D(z) = \begin{cases} \text{const} & z \le H_s/3 \\ z^{-1} & z \ge H_s/3, U_{10} < 7.5\text{m/s} \\ z^{-2} & z \ge H_s/3, U_{10} \ge 7.5\text{m/s} \end{cases} \tag{17}$$

The above relationship, together with measurements of the turbulent velocity spectrum at various depths within the water column provides the basis for estimating the dissipation for specific cases. Extension of such results to a relationship which can be used generally, requires an understanding of the functional dependence of these measured dissipation rates. These types of dependencies are presently being investigated. Examples of measured dissipation rates are presented later in this paper.

Bottom Friction

Direct measurements of the bottom friction dissipation in the field are very demanding and have not been attempted as part of the experiment. Rather, a detailed set of laboratory experiments have been conducted, in an effort to more fully understand the bottom friction source term under a spectrum of wind generated waves.

The bottom friction source term, $S_{bf}(f)$ is often represented in terms of the bottom shear stress τ_0 as:

$$S_{bf}(f) = -\left\langle \tau_0 u_b(f) \right\rangle \tag{18}$$

where u_b is the wave-induced bottom velocity. The bottom shear stress is further represented in terms of a quadratic friction law

$$\tau_0 = 0.5\rho_w f_w U_b^2 \tag{19}$$

where f_w is a bottom friction factor and U_b the maximum value of the bottom orbital velocity.

Mirfenderesk and Young (2001) [7] investigated the functional dependence of f_w using direct measurements of the bottom shear stress obtained with a mechanical shear plate. These measurements were conducted in a laboratory wave flume, with a number of difference bed roughness values. There results are broadly consistent with earlier results and can be summarized in the friction factor diagram in Figure 10.

Bottom material from the Lake George experimental site has been tested in the laboratory to determine typical values of the bed roughness k_s. This information, together with the results in Figure 10, provide sufficient information to determine the energy dissipation due to bottom friction.

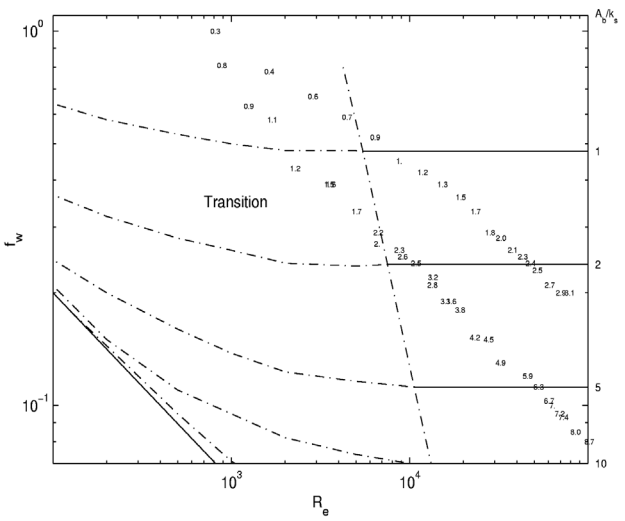

Figure 10. The friction factor results of Mirfenderesk and Young (2001) [7]. The figure shows the friction factor f_w as a function of the Reynolds Number R_e. The family of lines shown are from Jonsson (1966) [6] and are for constant values of A_b / k_s, where A_b is the bottom wave orbital excursion and k_s is the bed roughness. The numbers on the figure represent values of A_b / k_s obtained from the laboratory experimental data.

The Energy Balance

As the water depth at Lake George was quite shallow ($d < 0.5$ m), and the fetch was a number of kilometers, it is reasonable to assume the spectrum was in equilibrium and had reached a fully developed state. Hence, from (2) we obtain

$$\int S_{tot} df = 0 = \int S_{in} df + \int S_{wc} df + \int S_{bf} df \qquad (20)$$

That is, the total input should balance the total dissipation. Note that in (20), the nonlinear terms have been excluded as they are, by definition, conservative, with the integral always equalling zero.

As each of the terms in (20) can be calculated from the Lake George data, this relationship can be tested. The resulting balance is shown in Figure 11. The agreement is quite remarkable, considering the extremely complex nature of the experiments.

Conclusions

A detailed understanding of the many complex processes which are active in the generation and evolution of surface gravity waves will probably never be completely understood. Nevertheless, many activities require a level of understanding where predictions of wave conditions can be made with reasonable accuracy. The experimental projects described in this paper represent a body of more than 10 years of research, aimed at developing such an understanding. The data sets obtained during this extended experimental campaign are extensive and unique. The analysis of these data will involve many more years of work. Although the full analysis still awaits, progress has been considerable.

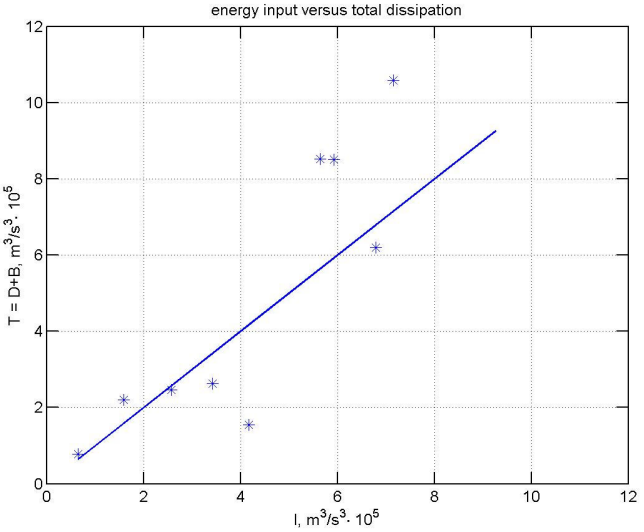

Figure 11. The total dissipation, (white-cap plus bottom friction) on the vertical axis, as a function of the total atmospheric input on the horizontal axis. As the waves are in equilibrium, these parameters should balance. The solid line shows this equilibrium. Data points are from Lake George.

A detailed understanding of the development of the directional spectrum under fetch-limited finite-depth conditions now exists. This understanding provides both a predictive capability (although it is largely empirical) and a "test bed" for the evaluation of theory.

Initial results aimed at determining the source terms responsible for the observed spectral evolution have been encouraging. The atmospheric input term has been parameterized to first order in terms of the environmental parameters. As well as a dependence on the speed of the wind relative to wave phase speed, wave breaking appears to also play a significant role. Atmospheric input is considerably enhanced above breaking waves, due to the atmospheric flow separation which occurs in such cases. A detailed representation of the magnitude of this enhancement is the subject of further analysis of the data.

A detailed study of the probability of breaking has shown that the modulation of waves within propagating groups plays a major role in determining whether breaking occurs. The probability of breaking has been parameterized in terms of a peak spectral steepness, shear in the water column and the relative water depth. The resulting relationship is capably of predicting breaking under a wide range of conditions.

Detailed measurements of the energy loss during breaking have been obtained from measurements of the turbulent velocity spectrum at various depths within the water column. These results look very encouraging and appear to confirm that in the severely depth-limited conditions of Lake George input is indeed balanced by dissipation. A detailed parameterization of the energy loss during breaking in terms of physical parameters is the subject of further analysis.

Acknowledgements

The Lake George project has been sponsored by both the Australian Research Council (ARC) and the US Office of Naval Research (ONR). This ongoing support is gratefully acknowledged.

References

[1] Banner, M.L., A.V. Babanin, and I.R. Young, Breaking Probability for Dominant Waves on the Sea Surface, *J. Phys. Oceanogr.*, **30**, 2000, 3145-3160.

[2] Babanin, A.V., I.R. Young, and M.L. Banner, Breaking Probabilities for Dominant Surface Waves on Water of Finite Constant Depth, *J. Geophys. Res.*, **106**, 2001, 11659-11676.

[3] Donelan, M.A., Wind-induced growth and attenuation of laboratory waves, in *Wind-over-Wave Couplings. Perspective and Prospects,* S.G.Sajadi, N.H.Thomas and J.C.R.Hunt, Eds., Clarendon Press, Oxford, 1999, 183-194.

[4] Gelci, R., J. Cazale, and J. Vassal, Utilisation des diagrammes de propagation a la provision energitique de la houle, *Bull. Inf. Comite Cen. Oceanogr. Etudes Cotes,* **8**, 1956, 169-187.

[5] Hasselmann, K. et al., Measurements of wind-wave growth and swell decay during the Joint North Sea Wave Project (JONSWAP), *Dtsch. Hydrogh. Z.*, Suppl. A, 8, **12**, 1973, 95pp.

[6] Jonsson, I.G., Wave boundary layer and friction factors, *Coastal Engineering Conf.* 1966.

[7] Mirfenderesk, H. and I.R. Young, Direct Measurements of the Bottom Friction Factor beneath Surface Gravity waves, 2001, *Coastal Eng*. (in press).

[8] Terray, E.A., M.A. Donelan, Y.C. Agrawal, W.M. Drennan, K.K. Kahma, A.J. Williams III, P.A. Hwang and S.A. Kitaigorodskii, Estimates of kinetic energy dissipation under breaking waves, *J. Phys. Oceanogr.*, **26,** 1996.

[9] Veron, F. and W.K. Melville, Pulse-to-pulse coherent Doppler measurements of waves and turbulence, *J. Atmos. Ocean Technology*, **16**, 1999, 1580-1597.

[10] The WAMDI Group (S. Hasselmann, K. Hasselmann, E. Bauer, P.A.E.M. Janssen, G.J. Komen, L. Bertotti, P. Lionello, A. Guallaume, V.C. Cardone, J.A. Greenwood, M. Reistad, L. Zambresky, and J.A. Ewing), The WAM model – a third generation ocean wave prediction model, *J. Phys. Oceanogr.*, **18**, 1988, 1775-1810.

[11] Wang, D.W., and P.A. Hwang, Evolution of the bimodal directional distribution of ocean waves, *J. Phys. Oceanogr.*, **31**, 2001, 1200-1221.

[12] Young, I.R., L.A. Verhagen, and M.L. Banner, A note on the bimodal directional spreading of fetch-limited wind waves., *J. Geophys. Res.*, **100**, 1995, 733-778.

[13] Young, I.R., and L.A. Verhagen, The growth of fetch limited waves in water of finite depth, part I, Total energy and peak frequency, *Coastal Eng.*, **29**, 1996a, 47-78.

[14] Young, I.R., and L.A. Verhagen, The growth of fetch limited waves in water of finite depth, part II, Spectral evolution, *Coastal Eng.*, **29**, 1996b, 79-100.

[15] Young, I.R., L.A. Verhagen, and S.K. Khatri, The growth of fetch limited waves in water of finite depth, part III, Directional spectra, *Coastal Eng.*, **29**, 1996, 101-121.